A BALANCING DOMAIN DECOMPOSITION BY CONSTRAINTS DELUXE METHOD FOR NUMERICALLY THIN REISSNER-MINDLIN PLATES APPROXIMATED WITH FALK-TU FINITE ELEMENTS TR2013-958

JONG HO LEE *

Abstract. The Reissner-Mindlin plate models thin plates. The condition numbers of finite element approximations of these plate models increase very rapidly as the thickness of the plate goes to 0. A Balancing Domain Decomposition by Constraints (BDDC) Deluxe method is developed for these plate problems discretized by Falk-Tu finite elements. In this new algorithm, subdomain Schur complements restricted to individual edges are used to define the average operator for the BDDC Deluxe method. It is established that the condition number of this preconditioned iterative method is bounded by $C(1+\log\frac{H}{h})^2$ if t, the thickness of the plate, is on the order of the element size h or smaller; H is the maximum diameter of the subdomains. The constant C is independent of the thickness t as well as H and h. Numerical results, which verify the theory, and a comparison with a traditional BDDC method are also provided.

Key words. domain decomposition, BDDC, preconditioners, iterative methods, Reissner-Mindlin plates, Falk-Tu elements, mixed finite element methods

AMS subject classifications. 65N55

1. Introduction.

The Reissner-Mindlin plate models the deformation of a thin plate under external forces; see [13, chapter 6.6] and [12, pp.195-232]. The thin plate is assumed to be of thickness t and its deformation is described by using two variables, the displacement, w, and the rotation, $\boldsymbol{\theta}$. In the limit case of $t = 0$, the Reissner-Mindlin plate model is identical to the Kirchhoff plate model, which requires the Kirchhoff condition, $\nabla w = \boldsymbol{\theta}$. It is also known that the solution of the Reissner-Mindlin plate model converges to that of the Kirchhoff plate model as the thickness of the plate decreases to zero; see [3] and [4].

If simple polynomial finite elements are used to discretize Reissner-Mindlin plates, we may suffer from locking problems because the Kirchhoff condition is too restrictive for low order polynomial finite elements. Thus, if continuous piecewise linear functions are used to approximate $\boldsymbol{\theta}$ and w with homogeneous boundary conditions, the finite element solution must vanish over the plate; see [12, pp.204]. By using mixed finite elements and a reduction operator Π on $\boldsymbol{\theta}$, locking problems can be avoided. We note that there are many good finite elements for Reissner-Mindlin plates; see e.g., [12, pp.195-232], [13, chapter 5.6], and [1, 2, 5–7, 15–18, 21, 22, 24, 29, 30, 32, 33].

Any Reissner-Mindlin plate problem without preconditioners has a condition number which is asymptotically proportional to

$$Ch^{-2}t^{-2},$$

where C is approximately 2 in our numerical experiments when h and t are small. Therefore, the condition number increases very rapidly as the thickness of a plate decreases and we need good preconditioners to obtain an efficient iterative solver for the Reissner-Mindlin plate problem.

* jlee@cims.nyu.edu This work has been supported by the National Science Foundation Grant DMS-0914954.

There are some previous studies on preconditioners of the Reissner-Mindlin plate problem. An overlapping domain decomposition method for the Reissner-Mindlin plate discretized by Falk-Tu finite elements is developed in [25, 26]. A BDDC method for the Reissner-Mindlin plate discretized by MITC elements is developed in [8–10]. A $C(H/h)$ bound on the condition number is obtained in [8] and improved to a $C(1+\log(H/h))^3$ bound in [9, 10]. A BDDC method for the Reissner-Mindlin plate discretized by Falk-Tu elements is suggested in [25] but without a proof of a strong condition number bound.

The BDDC Deluxe methods are variants of the traditional BDDC methods which use Schur complements restricted to individual faces to define the average operator instead of using a conventional pointwise average operator. Although this new average operator can be somewhat more expensive to apply, BDDC Deluxe methods provide better convergence rates than the traditional BDDC methods. The BDDC Deluxe methods were first developed by Dohrmann and Widlund; see [20]. Other applications of the BDDC Deluxe methods include [11] and [31].

Based on a BDDC method suggested in [25], a BDDC Deluxe method for the numerically thin Reissner-Mindlin plate discretized using Falk-Tu finite elements is developed in this paper and a condition number bound is established for the case when the plate thickness is on the order of the element size. A $C(1+\log(H/h))^2$ bound on the condition number is obtained and it shows at least as good results as those of [8–10, 26].

The Reissner-Mindlin plate theory and Falk-Tu finite elements are presented in section 2 and 3, respectively, following the presentation in [26]. Balancing domain decomposition by constraints Deluxe methods are introduced and their condition number bounds are proved in section 4. An energy bound for the dual variables and an edge lemma for the Reissner-Mindlin plate are given in section 5. Some numerical results on BDDC Deluxe methods and traditional BDDC methods are given in section 6. The estimated condition numbers for the new algorithm rarely exceed 4 for small values of t in our experiments.

2. The Continuous Problem. The plate is assumed to occupy the volume $P_t = \Omega \times (-\frac{t}{2}, +\frac{t}{2})$, where Ω is a bounded domain with unit diameter in $\mathbb{R}^2$ and t is the thickness of the plate. We are interested in the case when t is small. Under external forces, the plate is deformed and the displacement at each point can be described using three displacement variables u_i, $i = 1, 2, 3$. We assume the following four conditions on the displacement and the stress of the plate (see [13, chapter 6.5]):

H1. The linearity hypothesis.

H2. The displacement in the z-direction does not depend on the z-coordinate.

H3. The points on the middle surface are deformed only in the z-direction.

H4. The normal stress σ_{33} vanishes.

Under these four conditions, the displacement variables can be written as

$$\begin{aligned} u_i(x,y,z) &= -z\theta_i(x,y) \quad \text{for } i = 1,2, \\ u_3(x,y,z) &= w(x,y), \end{aligned}$$

in terms of w, the *displacement* variable, and $\boldsymbol{\theta} = (\theta_1, \theta_2)$, the *rotation*.

Using a reduction of dimension for the z-direction and the condition H4, the fol-

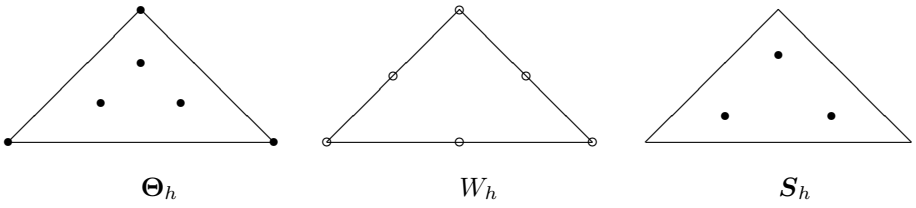

FIG. 3.1. *the Falk-Tu element with k=2.*

lowing variational problem is obtained: Minimize the Reissner-Mindlin energy

$$J(\boldsymbol{\theta}, w) = \frac{1}{2}\int_\Omega \boldsymbol{\mathcal{C}}\boldsymbol{\varepsilon}(\boldsymbol{\theta}) : \boldsymbol{\varepsilon}(\boldsymbol{\theta})\, dxdy + \frac{1}{2}\varrho t^{-2}\int_\Omega |\nabla w - \boldsymbol{\theta}|^2\, dxdy - \int_\Omega gw\, dxdy + \int_\Omega \boldsymbol{f}\cdot\boldsymbol{\theta}\, dxdy,$$

where $\varepsilon_{ij}(\boldsymbol{\theta}) = \frac{1}{2}\left(\frac{\partial\theta_i}{\partial x_j} + \frac{\partial\theta_j}{\partial x_i}\right)$, $\boldsymbol{\mathcal{C}}\boldsymbol{\varepsilon} = \frac{E}{1+\nu}(\boldsymbol{\varepsilon} + \frac{\nu}{1-\nu}trace(\boldsymbol{\varepsilon})\mathbf{I})$ with the two by two identity matrix $\mathbf{I}$, and $\boldsymbol{\varepsilon} : \boldsymbol{\sigma} = \sum_{ij}\varepsilon_{ij}\sigma_{ij}$. Here ν and E are the Lamé constants of linear elasticity and ϱ is another parameter related to the plate material. For simplicity, homogeneous Dirichlet boundary conditions are imposed on $\boldsymbol{\theta}$ and w.

If there were no essential boundary conditions, the null space of the Reissner-Mindlin energy is three dimensional and its basis elements are $w = 1$ and $\boldsymbol{\theta} = (0, 0)$, $w = x$ and $\boldsymbol{\theta} = (1, 0)$, and $w = y$ and $\boldsymbol{\theta} = (0, 1)$. The primal variables defined later will reproduce all functions in this null space.

If we approximate $\boldsymbol{\theta}$ and w directly using finite elements, there may be locking. These problems can be avoided by using mixed finite elements and introducing the shear stress variable $\boldsymbol{\gamma} := \varrho t^{-2}(\nabla w - \boldsymbol{\theta})$; see [8, 12], and [13, chapter 6.6]. After including the shear stress variable, we have the following variational problem: Find $\boldsymbol{\theta}_s \in \boldsymbol{H}_0^1(\Omega), w_s \in H_0^1(\Omega)$, and $\boldsymbol{\gamma}_s \in \boldsymbol{L}^2(\Omega)$ such that

$$\begin{aligned} a(\boldsymbol{\theta}_s, \boldsymbol{\phi}) + (\boldsymbol{\gamma}_s, \nabla v - \boldsymbol{\phi}) &= (g, v) - (\boldsymbol{f}, \boldsymbol{\phi}), \quad && \boldsymbol{\phi} \in \boldsymbol{H}_0^1(\Omega), v \in H_0^1(\Omega), \\ (\nabla w_s - \boldsymbol{\theta}_s, \boldsymbol{\eta}) - \varrho^{-1}t^2(\boldsymbol{\gamma}_s, \boldsymbol{\eta}) &= 0, && \boldsymbol{\eta} \in \boldsymbol{L}^2(\Omega), \end{aligned} \tag{2.1}$$

where $a(\boldsymbol{\theta}, \boldsymbol{\phi}) := \int_\Omega \boldsymbol{\mathcal{C}}\boldsymbol{\varepsilon}(\boldsymbol{\theta}) : \boldsymbol{\varepsilon}(\boldsymbol{\phi})\, dxdy$.

3. Discretization by Falk-Tu Elements. The Falk-Tu elements are conforming elements, i.e., $\boldsymbol{\Theta}_h \subset \boldsymbol{H}_0^1(\Omega)$, $W_h \subset H_0^1(\Omega)$, and $\boldsymbol{S}_h \subset \boldsymbol{L}^2(\Omega)$. We choose (see [12, 23])

$$\boldsymbol{\Theta}_h = \boldsymbol{M}_{1,0}^{k-1} + \boldsymbol{B}^{k+2},\ W_h = M_{1,0}^k,\ \boldsymbol{S}_h = \boldsymbol{M}_0^{k-1} \tag{3.1}$$

on the chosen triangulation with $k \geq 2$; see Figure 3.1 for the case of $k = 2$. Here $\boldsymbol{M}_{a,0}^k$ has components in the space of piecewise k-th order polynomials and belongs to $\boldsymbol{H}_0^a(\Omega)$, $M_{a,0}^k$ is the space of piecewise k-th order polynomials in $H_0^a(\Omega)$, $\boldsymbol{M}_a^k$ has components in the space of piecewise k-th order polynomials and belongs to $\boldsymbol{H}^a$, and $\boldsymbol{B}^k$ is the space of piecewise k-th order polynomial bubble functions. From now on, we will concentrate on Falk-Tu elements with $k = 2$.

Let Π be the $\boldsymbol{L}^2$ projector of $\boldsymbol{H}_0^1(\Omega)$ onto $\boldsymbol{S}_h$. We then have the following discrete

problem, as in [12,13]: Find $\boldsymbol{\theta}_h \in \boldsymbol{\Theta}_h, w_h \in W_h$, and $\boldsymbol{\gamma}_h \in \boldsymbol{S}_h$ such that

$$\begin{aligned} a(\boldsymbol{\theta}_h, \boldsymbol{\phi}_h) + (\boldsymbol{\gamma}_h, \nabla v_h - \Pi\boldsymbol{\phi}_h) &= (g, v_h) - (\boldsymbol{f}, \boldsymbol{\phi}_h), \quad \boldsymbol{\phi}_h \in \boldsymbol{\Theta}_h, v_h \in W_h, \\ (\nabla w_h - \Pi\boldsymbol{\theta}_h, \boldsymbol{\eta}_h) - \varrho^{-1}t^2(\boldsymbol{\gamma}_h, \boldsymbol{\eta}_h) &= 0, \qquad\qquad\qquad\quad \boldsymbol{\eta}_h \in \boldsymbol{S}_h. \end{aligned} \tag{3.2}$$

From Boffi et al. [12, pp.213-216], we have the following finite element error bound for the case of $k = 2$.

THEOREM 3.1. *For a sufficiently smooth solution of the continuous problem, we have*

$$\|\boldsymbol{\theta}_s - \boldsymbol{\theta}_h\|_0 + \|w_s - w_h\|_1 \leq Ch^2(\|\boldsymbol{f}\|_0 + \|g\|_0), \tag{3.3}$$

where C is independent of h.

Because we use stress variables which are discontinuous between elements, we can eliminate them on the element level as is also done in [8,19,26]. We then obtain the following discrete problem: Find $\boldsymbol{\theta}_h \in \boldsymbol{\Theta}_h$ and $w_h \in W_h$ such that

$$b((\boldsymbol{\theta}_h, w_h), (\boldsymbol{\phi}_h, v_h)) = (g, v_h) - (\boldsymbol{f}, \boldsymbol{\phi}_h), \quad \boldsymbol{\phi}_h \in \boldsymbol{\Theta}_h,\ v_h \in W_h, \tag{3.4}$$

where b is defined as

$$b((\boldsymbol{\theta}, w), (\boldsymbol{\phi}, v)) := a(\boldsymbol{\theta}, \boldsymbol{\phi}) + \frac{\varrho}{t^2}(\Pi\boldsymbol{\theta} - \nabla w, \Pi\boldsymbol{\phi} - \nabla v). \tag{3.5}$$

We now define $u := (\boldsymbol{\theta}, w)$ and $\widehat{\mathbf{U}} := \boldsymbol{\Theta}_h \times W_h$.

4. The BDDC Deluxe Algorithm.

4.1. Decomposition of the Domain. We assume that the domain Ω is decomposed into a set of shape-regular nonoverlapping open subdomains $\{\Omega_i\}_{i=1}^N$ with diameters H_i as in [13, 14, 34]. For simplicity, each subdomain is assumed to be a triangle; it is easy to extend our theory to polygonal subdomain cases given that a polygon is a union of triangles. Each subdomain Ω_i is then decomposed further using quasi-uniform and shape-regular finite elements with a minimum diameter h_i such that the nodes of the elements match across the interface between the subdomains. The maximum of $\frac{H_i}{h_i}, i = 1, \ldots, N$, will be denoted by $\frac{H}{h}$.

4.2. Primal and Dual Spaces. In the following, $\mathbf{U}^{(i)}$ will denote the vector space of values at the nodes of $\overline{\Omega}_i \setminus \partial\Omega$. Each $\mathbf{U}^{(i)}$ can be decomposed into a vector space of values at the subdomain *interface* nodes and a vector space of values at the subdomain *interior* nodes: $\mathbf{U}^{(i)} = \mathbf{U}_\Gamma^{(i)} \bigoplus \mathbf{U}_I^{(i)}$. The space of values at the subdomain interface nodes will be further decomposed into a space of the *primal* variables and a complementary space of *dual* variables: $\mathbf{U}_\Gamma^{(i)} = \mathbf{U}_\Pi^{(i)} \bigoplus \mathbf{U}_\Delta^{(i)}$.

The bases of the primal and dual spaces are assumed to have been transformed so that each primal constraint corresponds to an explicit primal variable of $\mathbf{U}_\Pi$ and $\mathbf{U}_\Delta$ consists of functions with vanishing primal constraints as in [28]. We assume that the interface space $\mathbf{U}_\Gamma^{(i)}$ has been transformed in the same way. The primal variables defined later will include nodal values at all the subdomain vertices and the dual variables will vanish at the vertices.

Related product spaces, which allow discontinuities across the interface, are denoted by

$$\mathbf{U} := \prod_{i=1}^{N} \mathbf{U}^{(i)}, \quad \mathbf{U}_\Gamma := \prod_{i=1}^{N} \mathbf{U}_\Gamma^{(i)}, \quad \mathbf{U}_I := \prod_{i=1}^{N} \mathbf{U}_I^{(i)},$$
$$\mathbf{U}_\Pi := \prod_{i=1}^{N} \mathbf{U}_\Pi^{(i)}, \qquad \text{and} \qquad \mathbf{U}_\Delta := \prod_{i=1}^{N} \mathbf{U}_\Delta^{(i)}.$$

Therefore, we also have $\mathbf{U} = \mathbf{U}_\Gamma \bigoplus \mathbf{U}_I$ and $\mathbf{U}_\Gamma = \mathbf{U}_\Pi \bigoplus \mathbf{U}_\Delta$.

The continuous subspace of $\mathbf{U}_\Gamma$ is denoted by $\widehat{\mathbf{U}}_\Gamma$ and the continuous subspace of $\mathbf{U}$ by $\widehat{\mathbf{U}}$. The finite element solution is continuous and belongs to $\widehat{\mathbf{U}}$. To describe BDDC methods, we also need a subspace $\widetilde{\mathbf{U}}_\Gamma \subset \mathbf{U}_\Gamma$ which allows discontinuities only for the dual variables and can be written as

$$\widetilde{\mathbf{U}}_\Gamma := \widehat{\mathbf{U}}_\Pi \bigoplus \mathbf{U}_\Delta = \widehat{\mathbf{U}}_\Pi \bigoplus \left(\prod_{i=1}^{N} \mathbf{U}_\Delta^{(i)} \right),$$

where $\widehat{\mathbf{U}}_\Pi$ is the continuous subspace of $\mathbf{U}_\Pi$. $\widehat{\mathbf{U}}_\Pi$ is related to a coarse-level, global problem of our iterative method.

As in [28], we define several restriction and extension operators for our BDDC method: $\widetilde{R}_\Gamma^{(i)} : \widetilde{\mathbf{U}}_\Gamma \to \mathbf{U}_\Gamma^{(i)}$, $\widetilde{R}_\Delta^{(i)} : \widetilde{\mathbf{U}}_\Gamma \to \mathbf{U}_\Delta^{(i)}$, $\widetilde{R}_\Pi^{(i)} : \widetilde{\mathbf{U}}_\Gamma \to \mathbf{U}_\Pi^{(i)}$, and $\widetilde{R}_\Pi : \widetilde{\mathbf{U}}_\Gamma \to \mathbf{U}_\Pi$ map $\widetilde{\mathbf{U}}_\Gamma$ to their corresponding components on $\Gamma^{(i)}$ and $\mathbf{U}_\Pi$, respectively. $\widehat{R}_\Gamma^{(i)} : \widehat{\mathbf{U}}_\Gamma \to \mathbf{U}_\Gamma^{(i)}$, $\widehat{R}_\Delta^{(i)} : \widehat{\mathbf{U}}_\Gamma \to \mathbf{U}_\Delta^{(i)}$, $\widehat{R}_\Pi^{(i)} : \widehat{\mathbf{U}}_\Gamma \to \mathbf{U}_\Pi^{(i)}$, and $\widehat{R}_\Pi : \widehat{\mathbf{U}}_\Gamma \to \widehat{\mathbf{U}}_\Pi$ map $\widehat{\mathbf{U}}_\Gamma$ to their corresponding components on $\Gamma^{(i)}$ and $\widehat{\mathbf{U}}_\Pi$, respectively. $\widetilde{R}_\Gamma : \widehat{\mathbf{U}}_\Gamma \to \widetilde{\mathbf{U}}_\Gamma$ is the direct sum of $\widehat{R}_\Pi$ and $\widehat{R}_\Delta^{(i)}, i = 1, \ldots, N$.

4.3. Discrete Harmonic Functions and Schur Complements. The bilinear form b related to the nodes of $\overline{\Omega}_i \setminus \partial\Omega$ and its right hand side can be represented in matrix form as follows:

$$\begin{bmatrix} B_{II}^{(i)} & B_{I\Gamma}^{(i)} \\ B_{\Gamma I}^{(i)} & B_{\Gamma\Gamma}^{(i)} \end{bmatrix} \begin{bmatrix} u_I^{(i)} \\ u_\Gamma^{(i)} \end{bmatrix} = \begin{bmatrix} f_I^{(i)} \\ f_\Gamma^{(i)} \end{bmatrix}.$$

If $u^{(i)}$ satisfies

$$B_{II}^{(i)} u_I^{(i)} + B_{I\Gamma}^{(i)} u_\Gamma^{(i)} = 0, \tag{4.1}$$

then $u^{(i)}$ is said to be a discrete harmonic function; see [34, chapter 4]. The interior values are well defined by solving the equation (4.1) with given subdomain interface values $u_\Gamma^{(i)}$, and this solution is denoted by $\mathcal{H}_i(u_\Gamma^{(i)})$ where $\mathcal{H}_i$ is the discrete harmonic extension operator into Ω_i. Note that a discrete harmonic function is orthogonal to any interior function on any subdomain in the sense of the b-bilinear form.

The Schur complement $S^{(i)}$ of $\mathbf{U}_\Gamma^{(i)}$ is defined as

$$S^{(i)} := B_{\Gamma\Gamma}^{(i)} - B_{\Gamma I}^{(i)} {B_{II}^{(i)}}^{-1} B_{I\Gamma}^{(i)}, \quad i = 1, ..., N. \tag{4.2}$$

If Ω_i is a floating subdomain, $S^{(i)}$ is singular with null space elements of zero b-bilinear energy.

The Schur complement S of the product space $\mathbf{U}_\Gamma$ is defined as the direct sum of the $S^{(i)}$. We define $\widehat{S} := \sum_{i=1}^{N} \widehat{R}_\Gamma^{(i)^T} S^{(i)} \widehat{R}_\Gamma^{(i)}$, which is the Schur complement S restricted to $\widehat{\mathbf{U}}_\Gamma$, and also define

$$\widetilde{S} := \sum_{i=1}^{N} \left[\widetilde{R}_\Pi^{(i)^T} \widetilde{R}_\Delta^{(i)^T} \right] S^{(i)} \begin{bmatrix} \widetilde{R}_\Pi^{(i)} \\ \widetilde{R}_\Delta^{(i)} \end{bmatrix} \tag{4.3}$$

$$= \left[\widetilde{R}_\Pi^{(i)^T} \widetilde{R}_\Delta^{(i)^T} \right] \begin{bmatrix} S_{\Pi\Pi}^{(i)} & S_{\Pi\Delta}^{(i)} \\ S_{\Delta\Pi}^{(i)} & S_{\Delta\Delta}^{(i)} \end{bmatrix} \begin{bmatrix} \widetilde{R}_\Pi^{(i)} \\ \widetilde{R}_\Delta^{(i)} \end{bmatrix}, \tag{4.4}$$

which is the Schur complement S restricted to $\widetilde{\mathbf{U}}_\Gamma$. Note that the Schur complement on $\widehat{\mathbf{U}}_\Gamma$ can be written as

$$\widehat{S} = \widetilde{R}_\Gamma^T \widetilde{S} \widetilde{R}_\Gamma. \tag{4.5}$$

Eliminating the interior equations of the original equation, we obtain the following global problem on the interface:

$$\widehat{S}_\Gamma u_\Gamma = g_\Gamma, \tag{4.6}$$

with

$$g_\Gamma = \sum_{i=1}^{N} \widehat{R}_\Gamma^{(i)^T} \left(f_\Gamma^{(i)} - B_{\Gamma I}^{(i)} B_{II}^{(i)^{-1}} f_I^{(i)} \right).$$

We will develop our BDDC Deluxe preconditioner for the operator of equation (4.6).

4.4. The Scaling Operator and the BDDC Deluxe Preconditioner. Any BDDC algorithm is defined by the choice of primal variables and the scaling operator that computes an average across the interface. We will first define the scaling operator $\widetilde{R}_{D,\Gamma}^T : \widetilde{\mathbf{U}}_\Gamma \to \widehat{\mathbf{U}}_\Gamma$.

Let e_{ij} be the edge between two subdomains Ω_i and Ω_j and E_{ij} be the set of the dual variables on e_{ij}. We obtain two principal minors of the Schur complements $S^{(i)}$ and $S^{(j)}$ by restricting them to E_{ij} and denote these two smaller matrices by $S_{E_{ij}}^{(i)}$ and $S_{E_{ij}}^{(j)}$. The average of $u \in \widetilde{\mathbf{U}}_\Gamma$ across the edge is then defined as

$$\bar{u}_{E_{ij}} := (S_{E_{ij}}^{(i)} + S_{E_{ij}}^{(j)})^{-1} (S_{E_{ij}}^{(i)} u_{E_{ij}}^{(i)} + S_{E_{ij}}^{(j)} u_{E_{ij}}^{(j)}). \tag{4.7}$$

All subdomain vertex variables will be included in the set of primal variables and the operator $\widetilde{R}_{D,\Gamma}^T$ is defined as the direct sum of these scaling operators on the dual variables and the operator $\widehat{R}_\Pi^T$ for the primal variables. As usual, $\widetilde{R}_{D,\Gamma}$ is the transpose of $\widetilde{R}_{D,\Gamma}^T$.

From these definitions, we easily see that

$$\widetilde{R}_\Gamma^T \widetilde{R}_{D,\Gamma} = \widetilde{R}_{D,\Gamma}^T \widetilde{R}_\Gamma = I. \tag{4.8}$$

We define the BDDC Deluxe preconditioner using $\widetilde{S}$ of (4.3) as

$$M_{\text{BDDC}}^{-1} := \widetilde{R}_{D,\Gamma}^T \widetilde{S}^{-1} \widetilde{R}_{D,\Gamma}. \tag{4.9}$$

4.5. A Stable Decomposition. From [26, subsection 5.2], we know that if u is discrete harmonic in each subdomain and t is on the order of h, or smaller than h, i.e., $t \leq Ch$, we can find $\widetilde{u} := (\widetilde{\boldsymbol{\theta}}, \widetilde{w})$ such that the Reissner-Mindlin energy of the two functions, u and $\widetilde{u}$, are equivalent. Here $\widetilde{u}$ is defined by $\widetilde{w} = w$, $\widetilde{\boldsymbol{\theta}}_L = \boldsymbol{\theta}_L$, and $\nabla\widetilde{w} = \Pi\widetilde{\boldsymbol{\theta}}$. In interesting problems of the Reissner-Mindlin plates, t is in this good range. If t is substantially larger than h, the error in the model may be larger than the finite element error. In the following, small t will mean that t is $t \leq Ch$.

4.6. A Condition Number Bound for the BDDC Deluxe Operator. Following the proofs in [27, 35, 36], we will establish a condition number bound of the BDDC Deluxe operator.

LEMMA 4.1. *The eigenvalues of the BDDC Deluxe operator are bounded from below by 1.*

Proof. For any given $u_\Gamma \in \widehat{\mathbf{U}}_\Gamma$, let $w_\Gamma := M_{\mathrm{BDDC}} u_\Gamma$. By (4.8), we have

$$\begin{aligned}
u_\Gamma^T M_{\mathrm{BDDC}} u_\Gamma &= u_\Gamma^T \widetilde{R}_\Gamma^T \widetilde{S} \widetilde{S}^{-1} \widetilde{R}_{D,\Gamma} w_\Gamma \\
&\leq \left(\widetilde{R}_\Gamma u_\Gamma, \widetilde{R}_\Gamma u_\Gamma\right)_{\widetilde{S}}^{1/2} \left(\widetilde{S}^{-1}\widetilde{R}_{D,\Gamma} w_\Gamma, \widetilde{S}^{-1}\widetilde{R}_{D,\Gamma} w_\Gamma\right)_{\widetilde{S}}^{1/2} \\
&= \left(u_\Gamma^T \widetilde{R}_\Gamma^T \widetilde{S} \widetilde{R}_\Gamma u_\Gamma\right)^{1/2} \left(w_\Gamma^T \widetilde{R}_{D,\Gamma}^T \widetilde{S}^{-1} \widetilde{S} \widetilde{S}^{-1} \widetilde{R}_{D,\Gamma} w_\Gamma\right)^{1/2} \\
&= \left(u_\Gamma^T \widehat{S} u_\Gamma\right)^{1/2} \left(u_\Gamma^T M_{\mathrm{BDDC}} M_{\mathrm{BDDC}}^{-1} M_{\mathrm{BDDC}} u_\Gamma\right)^{1/2} \\
&= \left(u_\Gamma^T \widehat{S} u_\Gamma\right)^{1/2} \left(u_\Gamma^T M_{\mathrm{BDDC}} u_\Gamma\right)^{1/2}.
\end{aligned}$$

Therefore, $u_\Gamma^T M_{\mathrm{BDDC}} u_\Gamma \leq u_\Gamma^T \widehat{S} u_\Gamma$. ∎

For the upper bound, we will prove the following two Lemmas in section 5 after that the primal variables have been defined.

LEMMA 4.2.

$$|u_\Pi^{(i)}|^2_{S_{\Pi\Pi}^{(i)}} \leq C(1 + \log\frac{H}{h})^2 |u_\Gamma^{(i)}|^2_{S^{(i)}}, \quad u_\Gamma^{(i)} \in \mathbf{U}_\Gamma^{(i)}, \tag{4.10}$$

where C is independent of H, h, and t if t is small.

The proof of Lemma 4.2 can be borrowed from [26] since the primal variables will be defined in a way similar to the coarse basis functions of an overlapping method in [26].

LEMMA 4.3.

$$|u_{E_{ij}}^{(i)}|^2_{S_{E_{ij}}^{(i)}} \leq C(1 + \log\frac{H}{h})^2 |u_\Gamma^{(i)}|^2_{S^{(i)}}, \quad u_\Gamma^{(i)} \in \mathbf{U}_\Gamma^{(i)}, \tag{4.11}$$

where C is independent of H, h, and t if t is small.

We now define an average operator $E_D : \widetilde{\mathbf{U}}_\Gamma \to \widehat{\mathbf{U}}_\Gamma \subset \widetilde{\mathbf{U}}_\Gamma$ by

$$E_D := \widetilde{R}_\Gamma \widetilde{R}_{D,\Gamma}^T. \tag{4.12}$$

Note that E_D is a projector and an identity operator on $\widehat{\mathbf{U}}_\Gamma$.

LEMMA 4.4.

$$|E_D u_\Gamma|^2_{\widetilde{S}} \leq C(1 + \log\frac{H}{h})^2 |u_\Gamma|^2_{\widetilde{S}}, \quad u_\Gamma \in \widetilde{\mathbf{U}}_\Gamma, \tag{4.13}$$

where C is independent of H, h, and t if t is small.

Proof.

$$|E_D u_\Gamma|^2_{\widetilde{S}} = \sum_{i=1}^{N} |\widetilde{R}^{(i)}_\Gamma E_D u_\Gamma|^2_{S^{(i)}} \tag{4.14}$$

$$\leq C \sum_{i=1}^{N} \left(|u^{(i)}_\Pi|^2_{S^{(i)}_{\Pi\Pi}} + |\widetilde{R}^{(i)}_\Gamma E_D (u_\Gamma - \widetilde{R}^T_\Pi u_\Pi)|^2_{S^{(i)}} \right). \tag{4.15}$$

We then have

$$\begin{aligned} |\widetilde{R}^{(i)}_\Gamma E_D (u_\Gamma - \widetilde{R}^T_\Pi u_\Pi)|^2_{S^{(i)}} &\leq C \sum_{j \in \Xi_i} |\bar{u}_{E_{ij}}|^2_{S^{(i)}_{E_{ij}}} \\ &\leq C \sum_{j \in \Xi_i} \left(|\bar{u}_{E_{ij}} - u^{(i)}_{E_{ij}}|^2_{S^{(i)}_{E_{ij}}} + |u^{(i)}_{E_{ij}}|^2_{S^{(i)}_{E_{ij}}} \right) \\ &\leq C|\Xi_i| \max_{j \in \Xi_i} \left(|\bar{u}_{E_{ij}} - u^{(i)}_{E_{ij}}|^2_{S^{(i)}_{E_{ij}}} + |u^{(i)}_{E_{ij}}|^2_{S^{(i)}_{E_{ij}}} \right), \end{aligned} \tag{4.16}$$

where Ξ_i is the set of j such that Ω_j has a common edge with Ω_i. Note that $|\Xi_i|$, the number of elements in Ξ_i, is bounded from above by three which is the maximum number of edges of any triangular subdomain.

The first term of (4.16) is bounded by

$$\begin{aligned} &|\bar{u}_{E_{ij}} - u^{(i)}_{E_{ij}}|^2_{S^{(i)}_{E_{ij}}} \\ &\quad = |(S^{(i)}_{E_{ij}} + S^{(j)}_{E_{ij}})^{-1} (S^{(j)}_{E_{ij}} u^{(j)}_{E_{ij}} - S^{(j)}_{E_{ij}} u^{(i)}_{E_{ij}})|^2_{S^{(i)}_{E_{ij}}} \\ &\quad \leq 2 {u^{(j)}_{E_{ij}}}^T S^{(j)}_{E_{ij}} (S^{(i)}_{E_{ij}} + S^{(j)}_{E_{ij}})^{-1} S^{(i)}_{E_{ij}} (S^{(i)}_{E_{ij}} + S^{(j)}_{E_{ij}})^{-1} S^{(j)}_{E_{ij}} u^{(j)}_{E_{ij}} \\ &\qquad + 2 {u^{(i)}_{E_{ij}}}^T S^{(j)}_{E_{ij}} (S^{(i)}_{E_{ij}} + S^{(j)}_{E_{ij}})^{-1} S^{(i)}_{E_{ij}} (S^{(i)}_{E_{ij}} + S^{(j)}_{E_{ij}})^{-1} S^{(j)}_{E_{ij}} u^{(i)}_{E_{ij}} \\ &\quad \leq 2 \left(|u^{(j)}_{E_{ij}}|^2_{S^{(j)}_{E_{ij}}} + |u^{(i)}_{E_{ij}}|^2_{S^{(i)}_{E_{ij}}} \right). \end{aligned} \tag{4.17}$$

From (4.15), (4.16), and (4.17), we then have

$$|E_D u_\Gamma|^2_{\widetilde{S}} \leq C \sum_{i=1}^{N} \left(|u^{(i)}_\Pi|^2_{S^{(i)}_{\Pi\Pi}} + |u^{(i)}_{E_{ij}}|^2_{S^{(i)}_{E_{ij}}} \right). \tag{4.18}$$

We then complete the proof by using Lemmas 4.2 and 4.3. ∎

Using Lemma 4.4, we have the following result.

LEMMA 4.5. *The eigenvalues of the BDDC Deluxe operator are bounded from above by $C(1 + \log(H/h))^2$ where C is independent of H, h, and t if t is small.*

Proof. Let again $w_\Gamma := M_{\mathrm{BDDC}} u_\Gamma$, as in the proof of Lemma 4.1, for any $u_\Gamma \in \widehat{\mathbf{U}}_\Gamma$.

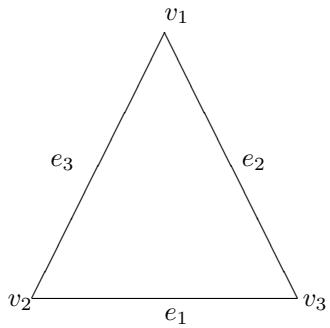

FIG. 5.1. *One subdomain and its vertices and edges.*

By Lemma 4.4, (4.8), (4.9), and (4.5), we have that

$$\begin{aligned}
u_\Gamma^T \widehat{S} u_\Gamma &= u_\Gamma^T \left(\widetilde{R}_\Gamma^T \widetilde{S} \widetilde{R}_\Gamma \right) M_{\mathrm{BDDC}}^{-1} w_\Gamma \\
&= \left(u_\Gamma^T \widetilde{R}_\Gamma^T \right) \widetilde{S} \left(\widetilde{R}_\Gamma \widetilde{R}_{D,\Gamma}^T \widetilde{S}^{-1} \widetilde{R}_{D,\Gamma} w_\Gamma \right) \\
&\leq \left(\widetilde{R}_\Gamma u_\Gamma, \widetilde{R}_\Gamma u_\Gamma \right)_{\widetilde{S}}^{1/2} \left(E_D \widetilde{S}^{-1} \widetilde{R}_{D,\Gamma} w_\Gamma, E_D \widetilde{S}^{-1} \widetilde{R}_{D,\Gamma} w_\Gamma \right)_{\widetilde{S}}^{1/2} \\
&\leq \left(u_\Gamma^T \widetilde{R}_\Gamma^T \widetilde{S} \widetilde{R}_\Gamma u_\Gamma \right)^{1/2} C(1 + \log \frac{H}{h}) \left(\widetilde{S}^{-1} \widetilde{R}_{D,\Gamma} w_\Gamma, \widetilde{S}^{-1} \widetilde{R}_{D,\Gamma} w_\Gamma \right)_{\widetilde{S}}^{1/2} \\
&= C(1 + \log \frac{H}{h}) \left(u_\Gamma^T \widehat{S} u_\Gamma \right)^{1/2} \left(u_\Gamma^T M_{\mathrm{BDDC}} \widetilde{R}_{D,\Gamma}^T \widetilde{S}^{-1} \widetilde{S} \widetilde{S}^{-1} \widetilde{R}_{D,\Gamma} M_{\mathrm{BDDC}} u_\Gamma \right)^{1/2} \\
&= C(1 + \log \frac{H}{h}) \left(u_\Gamma^T \widehat{S} u_\Gamma \right)^{1/2} \left(u_\Gamma^T M_{\mathrm{BDDC}} u_\Gamma \right)^{1/2}.
\end{aligned}$$

We then obtain $u_\Gamma^T \widehat{S} u_\Gamma \leq C(1 + \log(H/h))^2 u_\Gamma^T M_{\mathrm{BDDC}} u_\Gamma$. □

Therefore, we have the following bound for the condition number of our BDDC Deluxe operator.

THEOREM 4.6. *The condition number of the BDDC Deluxe operator satisfies the following bound*

$$\kappa(M_{\mathrm{BDDC}}^{-1} \widehat{S}) \leq C(1 + \log \frac{H}{h})^2,$$

where C is independent of H, h, and t if t is small.

5. The Primal Variables and Proofs of Lemmas 4.2 and 4.3.

5.1. The Definition of the Primal Variables. From now on, we consider mainly one of the floating subdomains Ω_l such that $\partial\Omega_l \bigcap \partial\Omega = \emptyset$. A set of indices for edges and vertices of Ω_l, e_1, e_2, e_3, v_1, v_2, and v_3, are defined by Figure 5.1. We now define our primal variables as being the same as the coarse basis functions in [26].

For θ_i, $i = 1, 2$, we define a rotational vertex primal variable which vanishes at all interface nodes except at one subdomain vertex v_k where its value equals $\theta_i(v_k)$. We denote these rotational vertex primal variables by $\boldsymbol{\theta}_{\Pi,i}^{v_k}$, $i = 1, 2$, $k = 1, 2, 3$. Since there are two components of $\boldsymbol{\theta}$, we have six rotational vertex primal variables for each subdomain.

We define a displacement vertex primal variable $w_\Pi^{v_k}$, $k = 1, 2, 3$, by giving w the value $w(v_k)$ at v_k, 0 at the other subdomain vertices, and making it linear along the edges of the subdomain. In addition to the definition of w on the interface, we give

values for θ_i on the two edges adjacent to the subdomain vertex being considered such that $\boldsymbol{\theta} = \frac{w(v_k)}{\ell_j}\mathbf{t}\psi_{e_j}$, where ℓ_j is the length of the edge e_j, $\mathbf{t}$ the unit tangent vector of the edge e_j from the vertex of the edge e_j other than v_k to v_k, and ψ_{e_j} the edge cut-off function which is a piecewise linear function defined on the edge and has values 1 at all interface nodes except at the two ends of the edge, where it vanishes.

We define a rotational edge primal variable $\boldsymbol{\theta}_\Pi^{e_k}$, $k = 1, 2, 3$, for each edge e_k by prescribing $\boldsymbol{\theta} = \bar{\boldsymbol{\theta}}_{e_k,\mathbf{n}}\mathbf{n}\psi_{e_k}$, where $\mathbf{n}$ is the unit normal vector of the edge e_k pointing into the right half plane and $\bar{\boldsymbol{\theta}}_{e_k,\mathbf{n}} := \int_{e_k}(I^h(\boldsymbol{\theta}\psi_{e_k})\cdot\mathbf{n})ds/\int_{e_k}\psi_{e_k}ds$. We set all the boundary values of w to zero.

$u_\Pi^{(l)}$ is the sum of the primal variables defined above:

$$u_\Pi^{(l)} = \sum_{k=1}^{3} w_\Pi^{v_k} + \sum_{k=1}^{3}\sum_{i=1}^{2}\boldsymbol{\theta}_{\Pi,i}^{v_k} + \sum_{k=1}^{3}\boldsymbol{\theta}_\Pi^{e_k}. \tag{5.1}$$

The dimension of the primal space per triangular subdomain is $9\times(1/6)+3\times(1/2) = 3$ on average. Note that $u_\Pi^{(l)}$ is continuous across the interface and that it is the coarse interpolant of an overlapping domain decomposition method for Reissner-Mindlin plates given by [26, (5.13)]. Lemma 4.2 is established in that paper; see [26, (5.17)].

Therefore, we only need to prove Lemma 4.3. For this, we need to borrow some results from [26].

5.2. Lemmas from [26]. Let ξ_1, ξ_2, and ξ_3 be the values of the barycentric functions of the subdomain at (x, y) related to e_1, e_2, and e_3, respectively. $\widetilde{\Omega}_l$ is defined as the union of Ω_l and its edges.

We define Υ_i on $\widetilde{\Omega}_l$ as follows:

$$\Upsilon_i := \frac{\xi_j^2\xi_k^2}{\xi_j^2\xi_k^2 + \xi_i^2\xi_j^2 + \xi_i^2\xi_k^2} \text{ on } \widetilde{\Omega}_l. \tag{5.2}$$

Note that Υ_i is equal to 1 on e_i and vanishes on the other edges. Υ_i has values between 0 and 1 and is not well defined at the vertices of Ω_l.

LEMMA 5.1. *The gradient of Υ_i is bounded by $\frac{C}{r}$ on any subdomain $\widetilde{\Omega}_l$ of diameter 1 where r is the minimum distance to the two vertices of the edge e_i. All the second order partial derivatives of the function Υ_i are bounded by $\frac{C}{r^2}$ on $\widetilde{\Omega}_l$.*

Proof. See the proof of [26, Lemma 5.2]. □

LEMMA 5.2. *The gradient of Υ_i, defined in (5.2), vanishes on the edges of the subdomain Ω_l.*

Proof. See the proof of [26, Lemma 5.3]. □

From [34, remark 4.13], we know that

$$||v||^2_{L^\infty(\Omega_l)} \le C(1+\log\frac{H_l}{h_l})||v||^2_{H^1(\Omega_l)}, \qquad v \in \boldsymbol{\Theta}_h|_{\overline{\Omega}_l} \text{ or } v \in W_h|_{\overline{\Omega}_l}. \tag{5.3}$$

From [26, (5.15)], we know that

$$|\bar{\boldsymbol{\theta}}_{e_k,\mathbf{n}}| = \left|\frac{\int_{e_k}(I^h(\boldsymbol{\theta}\psi_{e_k})\cdot\mathbf{n})ds}{\int_{e_k}\psi_{e_k}ds}\right| \le C||\boldsymbol{\theta}||_{H^1(\Omega_l)}. \tag{5.4}$$

LEMMA 5.3. *Under the condition $\Pi\widetilde{\boldsymbol{\theta}} = \nabla\widetilde{w}$, the b-seminorm and the H^1-seminorm are equivalent for $\widetilde{\boldsymbol{\theta}} \in \boldsymbol{\Theta}_h$. The constants of this equivalence do not depend on H_l*

and h_l but only on the shape regularity of the elements and the Lamé constants. In particular, we have the relation $|\widetilde{\boldsymbol{\theta}}|^2_{H^1(\Omega_l)} \leq Cb(\widetilde{\boldsymbol{\theta}}, \widetilde{\boldsymbol{\theta}})_{\Omega_l}$.

Proof. See the proof of [26, Lemma 5.8]. □

5.3. Proof of Lemma 4.3. We will use that $(\widetilde{\boldsymbol{\theta}}, \widetilde{w})$ has an energy equivalent to that of $u = (\boldsymbol{\theta}, w)$. Here we will drop the subscript ij and write e instead of e_{ij} and E instead of E_{ij}. We denote the two vertices of the edge e by v_1 and v_2. Without loss of generality, we assume that v_2 is at the origin, $(0, 0)$, and assume that the edge e can be expressed by $ax + by = 0$. Here, (a, b) is the unit tangent vector of e from v_2 to v_1. Let (a', b') be the unit normal vector of e pointing into the right half plane.

Define

$$\widetilde{w}_0 := \frac{w(v_1) - w(v_2)}{\ell}(ax + by) + w(v_2) + \bar{\boldsymbol{\theta}}_{e,\mathbf{n}}(a'x + b'y) \text{ on } \overline{\Omega}_l, \tag{5.5}$$

where ℓ is the length of the edge e. Note that $\widetilde{w}_0$ is linear and that $a'x + b'y$ vanishes on the edge e. We also define

$$\widetilde{\boldsymbol{\theta}}_0 := \nabla \widetilde{w}_0 \text{ on } \overline{\Omega}_l. \tag{5.6}$$

Note that $\widetilde{u}_0 := (\widetilde{\boldsymbol{\theta}}_0, \widetilde{w}_0)$ reproduces all functions in the null space of the Reissner-Mindlin energy. We can see, from (5.3) and (5.4), that

$$||\widetilde{w}_0||_{L^\infty(\Omega_l)} \leq C(||\widetilde{w}||_{L^\infty(\Omega_l)} + H_l||\widetilde{\boldsymbol{\theta}}||_{H^1(\Omega_l)}), \tag{5.7}$$

and

$$||\widetilde{\boldsymbol{\theta}}_0||_{L^\infty(\Omega_l)} = ||\nabla \widetilde{w}_0||_{L^\infty(\Omega_l)} \leq C(\frac{1}{H_l}||\widetilde{w}||_{L^\infty(\Omega_l)} + ||\widetilde{\boldsymbol{\theta}}||_{H^1(\Omega_l)}). \tag{5.8}$$

We then define

$$\bar{w} := \begin{cases} \widetilde{I^h}(\Upsilon(\widetilde{w} - \widetilde{w}_0)) & \text{at the nodes of } \widetilde{\Omega}_l, \\ 0 & \text{at the vertices of } \Omega_l, \end{cases} \tag{5.9}$$

and

$$\bar{\boldsymbol{\theta}}_L := \begin{cases} I^h(\nabla\Upsilon(\widetilde{w} - \widetilde{w}_0)) + I^h(\Upsilon(\widetilde{\boldsymbol{\theta}}_L - \nabla\widetilde{w}_0)) & \text{at the nodes of } \widetilde{\Omega}_l, \\ 0 & \text{at the vertices of } \Omega_l. \end{cases} \tag{5.10}$$

Then, these functions have the same interface values as $u_E^{(l)}$. Here $\widetilde{I^h}$ is the standard second order interpolation operator into M_1^2 and I^h is the standard first order interpolation operator into $\boldsymbol{M}_1^1$. We define the bubble functions by using the equation $\Pi\bar{\boldsymbol{\theta}} = \nabla\bar{w}$ on each element.

Note that $|\widetilde{w} - \tilde{w}_0|$ vanishes at the two vertices of the edge e and that $|\widetilde{w} - \tilde{w}_0|$ is bounded by

$$|\widetilde{w} - \tilde{w}_0| \leq r||\nabla(\widetilde{w} - \tilde{w}_0)||_{L^\infty(\Omega_l)} \tag{5.11}$$

$$\leq Cr(||\widetilde{\boldsymbol{\theta}}||_{L^\infty(\Omega_l)} + \frac{1}{H_l}||\widetilde{w}||_{L^\infty(\Omega_l)} + ||\widetilde{\boldsymbol{\theta}}||_{H^1(\Omega_l)}) \tag{5.12}$$

$$\leq Cr(1 + \log\frac{H_l}{h_l})^{\frac{1}{2}}(||\widetilde{\boldsymbol{\theta}}||_{H^1(\Omega_l)} + \frac{1}{H_l}||\widetilde{w}||_{H^1(\Omega_l)}), \tag{5.13}$$

where r is the minimum distance to the vertices of the edge e.

For each element K, which touches a subdomain vertex where $\bar{\boldsymbol{\theta}}$ vanishes, we have

$$|\bar{\boldsymbol{\theta}}|^2_{H^1(K)} \leq C\frac{1}{h^2}h^2||\bar{\boldsymbol{\theta}}||^2_{L^\infty(K)} \tag{5.14}$$

$$\leq C(||\bar{\boldsymbol{\theta}}_L||^2_{L^\infty(K)} + ||\nabla\bar{w}||^2_{L^\infty(K)}) \tag{5.15}$$

$$\leq C(1+\log\frac{H_l}{h_l})(||\widetilde{\boldsymbol{\theta}}||^2_{H^1(\Omega_l)} + \frac{1}{H_l^2}||\widetilde{w}||^2_{H^1(\Omega_l)}). \tag{5.16}$$

For each element K, which does not touch a subdomain vertex, we have

$$|\bar{\boldsymbol{\theta}}_L|^2_{H^1(K)} \leq \left|\left|\nabla^2\Upsilon(\widetilde{w}-\widetilde{w}_0)\right|\right|^2_{L^2(K)} + ||\nabla\Upsilon\nabla(\widetilde{w}-\widetilde{w}_0)||^2_{L^2(K)} + \left|\left|\nabla\Upsilon(\widetilde{\boldsymbol{\theta}}_L-\nabla\widetilde{w}_0)\right|\right|^2_{L^2(K)} + \left|\left|\Upsilon\nabla(\widetilde{\boldsymbol{\theta}}_L-\nabla\widetilde{w}_0)\right|\right|^2_{L^2(K)}. \tag{5.17}$$

Let $K(v)$ be the union of the elements K with one of its vertices in common with a vertex v of Ω_l. The sum of the first term of (5.17) over $\Omega_l \setminus K(v)$ is bounded by

$$\left|\left|\nabla^2\Upsilon(\widetilde{w}-\widetilde{w}_0)\right|\right|^2_{L^2(\Omega_l\setminus K(v))} \tag{5.18}$$

$$\leq C(||\widetilde{\boldsymbol{\theta}}||^2_{H^1(\Omega_l)} + \frac{1}{H_l^2}||\widetilde{w}||^2_{H^1(\Omega_l)})\int_0^{2\pi}\int_{ch_l}^{H_l}\frac{1}{r^4}(1+\log\frac{H_l}{h_l})r^2 r dr d\theta \tag{5.19}$$

$$\leq C(1+\log\frac{H_l}{h_l})^2(||\widetilde{\boldsymbol{\theta}}||^2_{H^1(\Omega_l)} + \frac{1}{H_l^2}||\widetilde{w}||^2_{H^1(\Omega_l)}). \tag{5.20}$$

The sum of the second term of (5.17) over $\Omega_l \setminus K(v)$ is bounded by

$$||\nabla\Upsilon\nabla(\widetilde{w}-\widetilde{w}_0)||^2_{L^2(\Omega_l\setminus K(v))}$$

$$\leq C(||\widetilde{\boldsymbol{\theta}}||^2_{H^1(\Omega_l)} + \frac{1}{H_l^2}||\widetilde{w}||^2_{H^1(\Omega_l)})\int_0^{2\pi}\int_{ch_l}^{H_l}\frac{1}{r^2}(1+\log\frac{H_l}{h_l})r dr d\theta$$

$$\leq C(1+\log\frac{H_l}{h_l})^2(||\widetilde{\boldsymbol{\theta}}||^2_{H^1(\Omega_l)} + \frac{1}{H_l^2}||\widetilde{w}||^2_{H^1(\Omega_l)}).$$

Similarly, the sum of the third term of (5.17) over $\Omega_l \setminus K(v)$ is bounded by

$$C(1+\log\frac{H_l}{h_l})^2(||\widetilde{\boldsymbol{\theta}}||^2_{H^1(\Omega_l)} + \frac{1}{H_l^2}||\widetilde{w}||^2_{H^1(\Omega_l)}).$$

Note that the second order derivatives of $\widetilde{w}_0$ vanishes because $\widetilde{w}_0$ is linear. Therefore, the fourth term of (5.17) is bounded by

$$\left|\left|\Upsilon\nabla(\widetilde{\boldsymbol{\theta}}_L-\nabla\widetilde{w}_0)\right|\right|^2_{L^2(K)} \leq \left|\left|\nabla\widetilde{\boldsymbol{\theta}}_L\right|\right|^2_{L^2(K)} \leq C||\widetilde{\boldsymbol{\theta}}||^2_{H^1(K)}.$$

For the bubble function $\bar{\boldsymbol{\theta}}_B$ of an element K, which does not touch a subdomain vertex, we know that

$$\Pi\bar{\boldsymbol{\theta}}_B = \nabla\bar{w} - \bar{\boldsymbol{\theta}}_L \tag{5.21}$$

$$= \nabla\left(\widetilde{I^h}(\Upsilon(\widetilde{w}-\widetilde{w}_0)) - (\Upsilon(\widetilde{w}-\widetilde{w}_0))\right) \tag{5.22}$$

$$+\nabla\left(\Upsilon(\widetilde{w}-\widetilde{w}_0)\right) - \left(I^h(\nabla\Upsilon(\widetilde{w}-\widetilde{w}_0)) + I^h(\Upsilon(\widetilde{\boldsymbol{\theta}}_L-\nabla\widetilde{w}_0))\right). \tag{5.23}$$

Therefore for each element K, which does not touch a subdomain vertex,

$$\begin{aligned}|\bar{\boldsymbol{\theta}}_B|^2_{H^1(K)} &\leq C||\bar{\boldsymbol{\theta}}_B||^2_{L^\infty(K)}\\ &\leq C\Bigg(||\nabla\left(\widetilde{I^h}(\Upsilon(\widetilde{w}-\widetilde{w}_0))-(\Upsilon(\widetilde{w}-\widetilde{w}_0))\right)||^2_{L^\infty(K)}\\ &\quad+||\nabla\Upsilon(\widetilde{w}-\widetilde{w}_0)-I^h(\nabla\Upsilon(\widetilde{w}-\widetilde{w}_0))||^2_{L^\infty(K)}\\ &\quad+||\Upsilon(\nabla\widetilde{w}-\nabla\widetilde{w}_0)-I^h(\Upsilon(\widetilde{\boldsymbol{\theta}}_L-\nabla\widetilde{w}_0))||^2_{L^\infty(K)}\Bigg). \qquad (5.24)\end{aligned}$$

We know that

$$||\nabla^2(\widetilde{w}-\widetilde{w}_0)||^2_{L^\infty(K)}=\frac{1}{h_l^2}||h_l^2\nabla^2\widetilde{w}||^2_{L^\infty(K)}\leq\frac{C}{h_l^2}||\nabla\widetilde{\boldsymbol{\theta}}||^2_{L^2(K)}. \qquad (5.25)$$

Using (5.7), (5.13), and (5.25), the sum of the first two terms of (5.24) of an element K of $\Omega_l\setminus K(v)$ is bounded by

$$\begin{aligned}&C\Bigg(||\nabla\left(\widetilde{I^h}(\Upsilon(\widetilde{w}-\widetilde{w}_0))-(\Upsilon(\widetilde{w}-\widetilde{w}_0))\right)||^2_{L^\infty(K)}\\ &\qquad+||\nabla\Upsilon(\widetilde{w}-\widetilde{w}_0)-I^h(\nabla\Upsilon(\widetilde{w}-\widetilde{w}_0))||^2_{L^\infty(K)}\Bigg)\\ &\leq Ch_l^2\left(||\nabla^2(\Upsilon(\widetilde{w}-\widetilde{w}_0))||^2_{L^\infty(K)}+||\nabla(\nabla\Upsilon(\widetilde{w}-\widetilde{w}_0))||^2_{L^\infty(K)}\right)\\ &\leq C(1+\log\frac{H_l}{h_l})(||\widetilde{\boldsymbol{\theta}}||^2_{H^1(\Omega_l)}+\frac{1}{H_l^2}||\widetilde{w}||^2_{H^1(\Omega_l)})\frac{h_l^2}{r^2}+C||\widetilde{\boldsymbol{\theta}}||^2_{H^1(K)}.\end{aligned}$$

The third term of (5.24) of an element K of $\Omega_l\setminus K(v)$ is bounded by

$$\begin{aligned}&C||\Upsilon(\nabla\widetilde{w}-\nabla\widetilde{w}_0)-I^h(\Upsilon(\widetilde{\boldsymbol{\theta}}_L-\nabla\widetilde{w}_0))||^2_{L^\infty(K)}\\ &\quad\leq C||\Upsilon(\nabla\widetilde{w}-\nabla\widetilde{w}_0)-I^h(\Upsilon(\nabla\widetilde{w}-\nabla\widetilde{w}_0))||^2_{L^\infty(K)}\\ &\qquad+C||I^h(\Upsilon(\nabla\widetilde{w}-\nabla\widetilde{w}_0))-I^h(\Upsilon(\widetilde{\boldsymbol{\theta}}_L-\nabla\widetilde{w}_0)||^2_{L^\infty(K)}\\ &\quad\leq Ch_l^2||\nabla(\Upsilon\nabla(\widetilde{w}-\widetilde{w}_0))||^2_{L^\infty(K)}+C||\nabla\widetilde{w}-\widetilde{\boldsymbol{\theta}}_L||^2_{L^\infty(K)}\\ &\quad\leq C(1+\log\frac{H_l}{h_l})(||\widetilde{\boldsymbol{\theta}}||^2_{H^1(\Omega_l)}+\frac{1}{H_l^2}||\widetilde{w}||^2_{H^1(\Omega_l)})\frac{h_l^2}{r^2}+C||\widetilde{\boldsymbol{\theta}}||^2_{H^1(K)}+C||\widetilde{\boldsymbol{\theta}}_B||^2_{L^\infty(K)}\\ &\quad\leq C(1+\log\frac{H_l}{h_l})(||\widetilde{\boldsymbol{\theta}}||^2_{H^1(\Omega_l)}+\frac{1}{H_l^2}||\widetilde{w}||^2_{H^1(\Omega_l)})\frac{h_l^2}{r^2}+C||\widetilde{\boldsymbol{\theta}}||^2_{H^1(K)}.\end{aligned}$$

There are on the order of $\frac{H_l^2}{h_l^2}$ elements in each subdomain and the number of elements with a distance r from a vertex is about $\frac{r}{h_l}$. Therefore, to bound $|\bar{\boldsymbol{\theta}}_B|^2_{H^1(\Omega_i)}$, we need to estimate

$$C\sum_{i=1}^{\frac{H_l}{h_l}}\frac{ih_l}{h_l}\frac{h_l^2}{i^2h_l^2}=C\sum_{i=1}^{\frac{H_l}{h_l}}\frac{h_l}{ih_l},$$

where $r = ih_l$. This sum is bounded by $C(1 + \log \frac{H_l}{h_l})$. Therefore,

$$|\bar{\boldsymbol{\theta}}_B|^2_{H^1(\Omega_l \setminus K(v))} \leq C(1 + \log \frac{H_l}{h_l})^2(||\widetilde{\boldsymbol{\theta}}||^2_{H^1(\Omega_l)} + \frac{1}{H_l^2}||\widetilde{w}||^2_{H^1(\Omega_l)}). \tag{5.26}$$

In total,

$$b(\bar{u}, \bar{u})_{\Omega_l} \leq C|\bar{\boldsymbol{\theta}}|^2_{H^1(\Omega_l)} \leq C(1 + \log \frac{H_l}{h_l})^2(||\widetilde{\boldsymbol{\theta}}||^2_{H^1(\Omega_l)} + \frac{1}{H_l^2}||\widetilde{w}||^2_{H^1(\Omega_l)}). \tag{5.27}$$

Because $\widetilde{u}_0$ reproduces $w = 1$ and $\boldsymbol{\theta} = (0, 0)$ which is in the null space of the Reissner-Mindlin energy, we have that

$$b(\bar{u}, \bar{u})_{\Omega_l} \leq C(1 + \log \frac{H_l}{h_l})^2||\widetilde{\boldsymbol{\theta}}||^2_{H^1(\Omega_l)}, \tag{5.28}$$

by using Poincaré's inequality and $|\widetilde{w}|^2_{H^1(\Omega_l)} \leq C||\widetilde{\boldsymbol{\theta}}||^2_{L^2(\Omega_l)}$ from $\nabla\widetilde{w} = \Pi\widetilde{\boldsymbol{\theta}}$.

By using Poincaré's inequality further with the other null space functions of the Reissner-Mindlin energy and Lemma 5.3,

$$b(\bar{u}, \bar{u})_{\Omega_l} \leq C(1 + \log \frac{H_l}{h_l})^2|\widetilde{\boldsymbol{\theta}}|^2_{H^1(\Omega_l)} \leq C(1 + \log \frac{H_l}{h_l})^2 b(u, u). \tag{5.29}$$

Because $\bar{u}$ has the same interface values as u_E, the values of the dual variables on the edge e, and that the harmonic extension minimizes the b-bilinear form energy, Lemma 4.3 is proved for a floating subdomain Ω_l.

If Ω_l is not a floating subdomain, we can modify the proof easily by using the same argument as in [26, subsection 5.4].

6. Numerical Experiments. In our numerical experiments, H is the coarse mesh size, h that of the fine mesh, and t the thickness of the plate. Experiments for each parameter set were run 50 times with random right hand sides and the average iteration counts and condition numbers are given. The stopping criteria for the conjugate gradient algorithm was $\frac{||r_n||_{l^2}}{||r_0||_{l^2}} \leq 10^{-6}$.

6.1. The BDDC Deluxe Operator. We have tested the BDDC Deluxe algorithm numerically using square subdomains.

The condition number as a function of the number of subdomains are given in Table 6.1; as expected, the condition number is bounded and it is also bounded for the case of a thick plate with $t = 1.0$.

Results with varying $\frac{H}{h}$ are given in Table 6.2 and Figure 6.1.

We can see that the maximum eigenvalue of the BDDC Deluxe operator is approximately proportional to $(1 + \log \frac{H}{h})^2$.

In numerical experiments with an overlapping Schwarz method in [26], the dimension of coarse space per subdomain was on average 7. The dimension of primal space per subdomain is on average 5 for our BDDC algorithm. In spite thereof, the condition number of our BDDC algorithm is smaller than that of our overlapping method.

6.2. The Traditional BDDC Operator. We have also tested the traditional BDDC operator numerically using square subdomains with the same parameters. The condition number as a function of the number of subdomains are given in Table 6.3. Results with varying $\frac{H}{h}$ are given in Table 6.4.

We can see that as the thickness of the plate t decreases and $\frac{H}{h}$ increases, the BDDC Deluxe preconditioner performs better than the traditional BDDC preconditioner.

TABLE 6.1
Results for the BDDC Deluxe preconditioner for $\frac{H}{h} = 4$, *decreasing* $h = \frac{1}{n}$, *and increasing the number of subdomains* $= \frac{n}{4} \times \frac{n}{4}$.

Number of Subdomains	λ_{max}	iter	λ_{max}	iter	λ_{max}	iter	λ_{max}	iter	λ_{max}	iter	λ_{max}	iter
	$t = 1.0$		$t = 10^{-1}$		$t = 10^{-2}$		$t = 10^{-3}$		$t = 10^{-4}$		$t = 10^{-5}$	
9	2.20	8.0	2.38	9.5	3.02	11.4	2.89	11.8	2.89	11.8	2.86	11.8
36	2.84	11.0	2.71	11.1	3.31	13.0	3.02	13.0	3.02	13.0	3.02	13.0
81	2.97	12.0	2.83	12.0	3.15	13.0	3.07	14.0	3.05	14.0	3.05	14.0
144	3.02	12.0	2.87	12.0	2.94	13.0	3.09	14.0	3.05	14.0	3.06	14.0
225	3.06	12.1	2.90	12.9	2.86	12.8	3.13	14.0	3.06	14.0	3.06	14.0
324	3.07	13.0	2.91	13.0	2.83	13.0	3.17	14.0	3.06	14.0	3.06	14.0
441	3.07	13.0	2.92	13.0	2.81	13.0	3.20	14.5	3.06	14.0	3.06	14.0
576	3.08	13.0	2.92	13.0	2.79	13.0	3.24	15.0	3.06	14.2	3.06	14.2
729	3.08	13.0	2.92	13.0	2.79	13.0	3.27	15.0	3.06	15.0	3.06	15.0
900	3.09	13.0	2.93	13.0	2.80	13.0	3.31	15.0	3.06	15.0	3.06	15.0

TABLE 6.2
Results for the BDDC Deluxe preconditioner for $h = \frac{1}{n}$, 4×4 *subdomains, and increasing* $\frac{H}{h} = \frac{n}{4}$.

H/h	λ_{max}	iter	λ_{max}	iter	λ_{max}	iter	λ_{max}	iter	λ_{max}	iter	λ_{max}	iter
	$t = 1.0$		$t = 10^{-1}$		$t = 10^{-2}$		$t = 10^{-3}$		$t = 10^{-4}$		$t = 10^{-5}$	
3	2.25	8.1	2.21	9.9	2.99	12.0	2.88	12.0	2.88	12.0	2.89	12.1
6	3.00	10.0	3.00	11.0	3.56	13.0	2.98	13.0	2.97	13.0	2.97	13.0
9	3.61	11.0	3.51	12.0	3.97	14.0	3.12	13.0	3.07	13.0	3.08	13.0
12	3.94	12.0	3.93	13.0	4.32	14.9	3.30	13.4	3.21	13.5	3.21	13.7
15	4.30	13.0	4.22	13.3	4.57	15.6	3.49	14.0	3.35	14.0	3.36	14.0
18	4.61	13.0	4.51	14.0	4.80	16.0	3.66	14.4	3.47	14.8	3.48	14.9
21	4.89	14.0	4.76	14.1	4.97	16.0	3.82	15.0	3.60	15.0	3.58	15.0
24	5.05	14.0	4.95	14.5	5.13	16.3	3.95	15.0	3.68	15.0	3.68	15.0
27	5.30	14.9	5.16	14.9	5.25	16.9	4.09	15.5	3.76	15.5	3.78	15.3
30	5.54	15.0	5.28	15.1	5.39	17.0	4.23	15.9	3.85	16.0	3.87	16.0

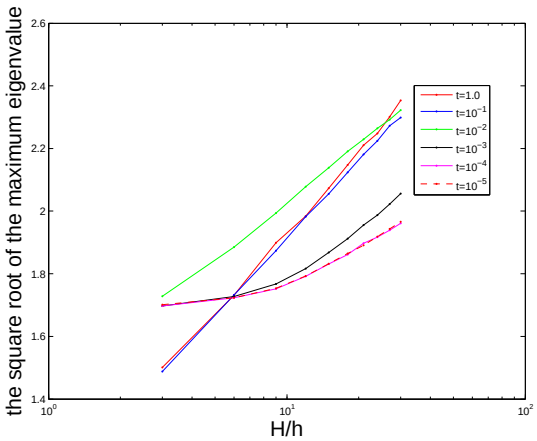

FIG. 6.1. *The square root of the maximum eigenvalue of the BDDC Deluxe operator as a function of* $\frac{H}{h}$.

TABLE 6.3
Results for the traditional BDDC preconditioner for $\frac{H}{h} = 4$, decreasing $h = \frac{1}{n}$, and increasing the number of subdomains $= \frac{n}{4} \times \frac{n}{4}$.

Number of Subdomains	λ_{max}	iter	λ_{max}	iter	λ_{max}	iter	λ_{max}	iter	λ_{max}	iter	λ_{max}	iter
	$t = 1.0$		$t = 10^{-1}$		$t = 10^{-2}$		$t = 10^{-3}$		$t = 10^{-4}$		$t = 10^{-5}$	
9	2.20	7.9	2.32	9.9	3.26	13.0	3.53	14.0	3.52	14.0	3.52	14.0
36	2.84	11.0	2.71	11.0	3.24	14.0	3.64	15.0	3.65	15.0	3.66	15.0
81	2.96	12.0	2.81	12.0	3.04	13.0	3.64	16.0	3.68	16.0	3.68	16.0
144	3.01	12.0	2.88	12.0	2.84	13.0	3.62	16.0	3.68	16.0	3.68	16.0
225	3.05	13.0	2.91	12.0	2.77	12.6	3.59	16.0	3.69	16.0	3.68	16.0
324	3.07	13.0	2.93	13.0	2.77	13.0	3.56	16.0	3.68	16.2	3.69	16.3
441	3.08	13.0	2.93	13.0	2.77	13.0	3.52	16.0	3.69	17.0	3.69	17.0
576	3.09	13.0	2.93	13.0	2.78	13.0	3.49	16.0	3.69	17.0	3.69	17.0
729	3.09	13.0	2.94	13.0	2.79	13.0	3.45	16.0	3.68	17.0	3.69	17.0
900	3.09	13.0	2.94	13.0	2.81	13.0	3.41	16.0	3.68	17.0	3.69	17.0

TABLE 6.4
Results for the traditional BDDC preconditioner for $h = \frac{1}{n}$, 4×4 subdomains, and increasing $\frac{H}{h} = \frac{n}{4}$.

H/h	λ_{max}	iter	λ_{max}	iter	λ_{max}	iter	λ_{max}	iter	λ_{max}	iter	λ_{max}	iter
	$t = 1.0$		$t = 10^{-1}$		$t = 10^{-2}$		$t = 10^{-3}$		$t = 10^{-4}$		$t = 10^{-5}$	
3	2.26	8.0	2.24	10.0	3.09	13.0	3.25	13.7	3.27	13.8	3.27	13.8
6	3.03	10.0	3.01	11.0	3.63	14.0	3.87	16.0	3.90	16.0	3.89	16.0
9	3.53	11.3	3.54	12.2	4.20	15.0	4.02	16.2	4.10	16.8	4.09	16.7
12	3.94	12.0	3.94	13.0	4.58	15.9	4.25	17.0	4.27	17.0	4.27	17.0
15	4.26	13.0	4.31	14.0	4.84	16.0	4.50	17.1	4.51	17.9	4.51	17.9
18	4.58	14.0	4.59	14.0	5.09	16.4	4.73	18.0	4.69	18.0	4.69	18.0
21	4.80	14.5	4.87	14.4	5.29	16.9	4.96	18.0	4.85	18.8	4.85	18.8
24	5.03	15.0	5.08	15.0	5.46	17.0	5.22	18.8	5.03	19.0	5.03	19.0
27	5.25	15.0	5.28	15.0	5.60	17.0	5.45	19.0	5.16	19.7	5.16	19.7
30	5.39	15.0	5.49	15.3	5.78	17.3	5.67	19.0	5.28	20.0	5.28	20.0

7. Acknowledgement. The author wishes to thank Prof. Olof Widlund of the Courant Institute, who made him aware of BDDC Deluxe and its possible use in this application. He also was helpful in organizing and commenting on drafts of this paper.

REFERENCES

[1] Douglas N. Arnold, Franco Brezzi, Richard S. Falk, and L. Donatella Marini. Locking-free Reissner-Mindlin elements without reduced integration. *Comput. Methods Appl. Mech. Engrg.*, 196(37-40):3660–3671, 2007.
[2] Douglas N. Arnold and Richard S. Falk. A uniformly accurate finite element method for the Reissner-Mindlin plate. *SIAM J. Numer. Anal.*, 26(6):1276–1290, 1989.
[3] Douglas N. Arnold and Richard S. Falk. The boundary layer for the Reissner-Mindlin plate model. *SIAM J. Math. Anal.*, 21(2):281–312, 1990.
[4] Douglas N. Arnold and Richard S. Falk. Asymptotic analysis of the boundary layer for the Reissner-Mindlin plate model. *SIAM J. Math. Anal.*, 27(2):486–514, 1996.
[5] Ferdinando Auricchio and Carlo Lovadina. Analysis of kinematic linked interpolation methods for Reissner-Mindlin plate problems. *Comput. Methods Appl. Mech. Engrg.*, 190(18-

19):2465–2482, 2001.

[6] Klaus-Jürgen Bathe and Franco Brezzi. On the convergence of a four-node plate bending element based on Mindlin-Reissner plate theory and a mixed interpolation. In *The mathematics of finite elements and applications, V (Uxbridge, 1984)*, pages 491–503. Academic Press, London, 1985.

[7] Lourenço Beirão da Veiga. Finite element methods for a modified Reissner-Mindlin free plate model. *SIAM J. Numer. Anal.*, 42(4):1572–1591 (electronic), 2004.

[8] Lourenço Beirão da Veiga, Claudia Chinosi, Carlo Lovadina, and Luca F. Pavarino. Robust BDDC preconditioners for Reissner-Mindlin plate bending problems and MITC elements. *SIAM J. Numer. Anal.*, 47(6):4214–4238, 2010.

[9] Lourenço Beirão da Veiga, Claudia Chinosi, Carlo Lovadina, Luca F. Pavarino, and Joachim Schöberl. Quasi-optimality of BDDC methods for MITC Reissner-Mindlin problems. In *Proceedings of the 20th International Conference on Domain Decomposition Methods*, 2011. Held in San Diego, CA, February 7-11, 2011. To appear.

[10] Lourenço Beirão da Veiga, Claudia Chinosi, Carlo Lovadina, Luca F. Pavarino, and Joachim Schöberl. Quasi-uniformity of BDDC preconditioners for the MITC Reissner-Mindlin problem. Technical Report 4PV11/2/0, I.M.A.T.I.-C.N.R., 2011.

[11] Lourenço Beirão da Veiga, Luca F. Pavarino, Simone Scacchi, Olof B. Widlund, and Stefano Zampini. Isogeometric BDDC preconditioners with deluxe scaling. Technical Report TR2013-955, Courant Institute, New York University, April 2013.

[12] Daniele Boffi, Franco Brezzi, Leszek F. Demkowicz, Ricardo G. Durán, Richard S. Falk, and Michel Fortin. *Mixed finite elements, compatibility conditions, and applications*, volume 1939 of *Lecture Notes in Mathematics*. Springer-Verlag, Berlin, 2008. Lectures given at the C.I.M.E. Summer School held in Cetraro, June 26–July 1, 2006, Edited by Daniele Boffi and Lucia Gastaldi.

[13] Dietrich Braess. *Finite elements*. Cambridge University Press, Cambridge, third edition, 2007. Theory, fast solvers, and applications in elasticity theory, Translated from the German by Larry L. Schumaker.

[14] Susanne C. Brenner and L. Ridgway Scott. *The mathematical theory of finite element methods*, volume 15 of *Texts in Applied Mathematics*. Springer, New York, third edition, 2008.

[15] Franco Brezzi, Klaus-Jürgen Bathe, and Michel Fortin. Mixed-interpolated elements for Reissner-Mindlin plates. *Internat. J. Numer. Methods Engrg.*, 28(8):1787–1801, 1989.

[16] Franco Brezzi, Michel Fortin, and Rolf Stenberg. Error analysis of mixed-interpolated elements for Reissner-Mindlin plates. *Math. Models Methods Appl. Sci.*, 1(2):125–151, 1991.

[17] Dominique Chapelle and Rolf Stenberg. An optimal low-order locking-free finite element method for Reissner-Mindlin plates. *Math. Models Methods Appl. Sci.*, 8(3):407–430, 1998.

[18] Claudia Chinosi, Carlo Lovadina, and L. Donatella Marini. Nonconforming locking-free finite elements for Reissner-Mindlin plates. *Comput. Methods Appl. Mech. Engrg.*, 195(25-28):3448–3460, 2006.

[19] Clark R. Dohrmann and Olof B. Widlund. An overlapping Schwarz algorithm for almost incompressible elasticity. *SIAM J. Numer. Anal.*, 47(4):2897–2923, 2009.

[20] Clark R. Dohrmann and Olof B. Widlund. Some recent tools and a BDDC algorithm for 3D problems in H(curl). In *Proceedings of the 20th International Conference on Domain Decomposition Methods*, 2011. Held in San Diego, CA, February 7-11, 2011. To appear.

[21] Ricardo G. Durán, Erwin Hernández, Luis Hervella-Nieto, Elsa Liberman, and Rodolfo Rodríguez. Error estimates for low-order isoparametric quadrilateral finite elements for plates. *SIAM J. Numer. Anal.*, 41(5):1751–1772 (electronic), 2003.

[22] Ricardo G. Durán and Elsa Liberman. On mixed finite element methods for the Reissner-Mindlin plate model. *Math. Comp.*, 58(198):561–573, 1992.

[23] Richard S. Falk and Tong Tu. Locking-free finite elements for the Reissner-Mindlin plate. *Math. Comp.*, 69(231):911–928, 2000.

[24] Alexander Iosilevich, Klaus-Jürgen Bathe, and Franco Brezzi. Numerical inf-sup analysis of MITC plate bending elements. In *Plates and shells (Québec, QC, 1996)*, volume 21 of *CRM Proc. Lecture Notes*, pages 225–242. Amer. Math. Soc., Providence, RI, 1999.

[25] Jong Ho Lee. *Domain Decomposition Methods for Reissner-Mindlin Plates Discretized with the Falk-Tu Elements.* PhD thesis, Courant Institute of Mathematical Sciences, New York, N.Y., 2011.

[26] Jong Ho Lee. Overlapping domain decomposition methods for numerically thin Reissner-Mindlin plates approximated with the Falk-Tu elements. *SIAM J. Numer. Anal.*, 51(1):24–46 (electronic), 2013.

[27] Jing Li and Olof Widlund. BDDC algorithms for incompressible Stokes equations. *SIAM J. Numer. Anal.*, 44(6):2432–2455, 2006.

[28] Jing Li and Olof B. Widlund. FETI-DP, BDDC, and block Cholesky methods. *Internat. J. Numer. Methods Engrg.*, 66(2):250–271, 2006.

[29] Carlo Lovadina. A new class of mixed finite element methods for Reissner-Mindlin plates. *SIAM J. Numer. Anal.*, 33(6):2457–2467, 1996.

[30] Mikko Lyly. On the connection between some linear triangular Reissner-Mindlin plate bending elements. *Numer. Math.*, 85(1):77–107, 2000.

[31] Duk-Soon Oh, Olof B. Widlund, and Clark R. Dohrmann. A BDDC algorithm for Raviart-Thomas vector fields. Technical Report TR2013-951, Courant Institute, New York University, February 2013.

[32] Petra Peisker and Dietrich Braess. Uniform convergence of mixed interpolated elements for Reissner-Mindlin plates. *RAIRO Modél. Math. Anal. Numér.*, 26(5):557–574, 1992.

[33] Rolf Stenberg. A new finite element formulation for the plate bending problem. In *Asymptotic methods for elastic structures (Lisbon, 1993)*, pages 209–221. de Gruyter, Berlin, 1995.

[34] Andrea Toselli and Olof B. Widlund. *Domain decomposition methods—algorithms and theory*, volume 34 of *Springer Series in Computational Mathematics*. Springer-Verlag, Berlin, 2005.

[35] Xuemin Tu. Three-level BDDC in three dimensions. *SIAM J. Sci. Comput.*, 29(4):1759–1780, 2007.

[36] Xuemin Tu. Three-level BDDC in two dimensions. *Internat. J. Numer. Methods Engrg.*, 69(1):33–59, 2007.